Magma mixing in the ophiolite: in the case of Ibara ophiolite, Southwest Japan

Yoshiyuki Koide
(Kanagawa Prefectural Museum)

オフィオライトにおけるマグマ・ミキシング 西南日本井原オフィオライトの例

小 出 良 幸
(神奈川県立博物館)

井原オフィオライトの噴出相の変玄武岩は，MORB 類似のソレアイトである。井原変玄武岩は，斑晶組み合せによって，3つのタイプに区分できる。3つのタイプの成因関係は，マグマ·ミキシングによって説明できる。SO type と呼ぶ未分化なマグマ（スピネル，カンラン石，斜長石が晶出）が，しばしば PC&NP type と呼ぶ分化したマグマ溜り（斜長石，単斜輝石，カンラン石が晶出）に注入された。TR type と呼ぶミキシングしたマグマは，Cr_2O_3 に富んでくる。Cr_2O_3 の増加によってスピネルの初相領域が広がり，TiO_2 に富んだスピネルが斜長石，単斜輝石，カンラン石に一緒に晶出し始める。TR type の単斜輝石に認められる波状逆累帯構造は，このようなミキシングのシナリオを支持している。

Abstract The Ibara metabasalt, effusive member of the Ibara ophiolite, is a MORB-like tholeiite, which is classified into three rock types with phenocryst assemblage. Genetic relationship among these rock types can be explained in term of magma mixing. The unfractionated primordial magma (SO type), which was crystallizing spinel, olivine and plagioclase, sometimes refill magma chamber (PC&NP type), where the fractionated magma was crystallizing plagioclase, clinopyroxene and olivine. The enfilled magma had been mixed with the fractionated magma. The mixed magma (TR type) became to be enriched in Cr_2O_3. Effect of Cr_2O_3 enrichment expanded spinel liquidus field. Consequently, the TR type magma started the crystallization of high-TiO_2 spinel together with plagioclase, clinopyroxene and olivine. The oscillatory reverse compositional zoning in clinopyroxene of the TR type metabasalt supports above the mixing scenario.

I. Introduction

O'HARA (1977) proposed the open magma chamber model of mid-ocean ridge basalt, that less fractionated magma successively injects into fractionating magma chamber in steady state. This magma mixing model in MORB is supported by various evidence (e.g., DONALDSON and BROWN, 1977; DUNGAN and RHODES, 1978; RHODES et al., 1979; WALKER et al., 1979). The crystallization process of ophiolitic basalts, most of which are fragments of an ancient oceanic crust, has not been clear, because their original rock and mineral chemistries usually have been modified as a result of metamorphism and alteration, such as ocean floor metamorphism, ocean floor weathering, and metamorphism during or after emplacement. Many studies on tectonic setting of ophiolitic basalts have been made using chemical affinity of immobile elements to recent oceanic basalt (e.g., BASS et al., 1973; MIYASHIRO, 1975; PEARCE et al., 1975, 1977). Although the Ibara metabasalt has been affected by metamorphism and alteration, the primary mineral phases, such as clinopyroxene and spinel, and igneous textures are preserved. In this paper, the author investigated field occurrence, mineral phase assemblage, relict mineral chemistry and immobile element abundances, and showed the information possible to make clear the crystallization and magma mixing processes similar to O'HARA (1977)'s open magma chamber model. This method may be adapted for other ophiolites and is useful to identify the magmatic processes of ophiolites.

II. Geologic Outline

The Maizuru Tectonic Belt is located between the Permian (HASE, 1964) and the Jurassic accretion complexes (HASHIMOTO, 1972; HASHIMOTO and SAITO, 1976; ISHIGA, 1983, 1985a, b, 1986a, b; CARIDROIT et al., 1985) in the Inner Zone of Southwest Japan. This tectonic belt consists of Late Carboniferous and Early Permian ophiolites (KOIDE et al., 1987), which are overlain by terrestrial sedimentary rocks of Late Permian and Triassic age.

The late Paleozoic ophiolite in the Ibara area belongs to the western extension of the Maizuru Tectonic Belt. The ophiolite is composed of Lower, Middle and Upper Members in ascending order, with accessory metagabbro and ultramafics. Three members and plutonic rocks are in fault contact with each other. These members are general E–W strike and dip homoclinally about 40° N (Fig. 1). In the southeastern margin of the area, these members are intruded by Cretaceous granite and are overlain by Cretaceous rhyolite.

Lower Member: The Lower Member is up to 1000 m thick. The lower part of this member is intruded by a granitic stock and affected by contact metamorphism. This member consists mainly of metabasalt with small amounts of hyaloclastite and intercalated black slate.

Middle Member: The black and massive slate intercalated with a few beds of conglomerate and metabasalt is the dominant rock type of the Middle Member which is up to 800 m thick. The conglomerate consists of subrounded to angular cobbles and pebbles of various rocks such as granite, diorite, metagabbro, metabasalt, arkorse sandstone, volcanic sandstone, and slate. These fragments are poorly sorted, and a muddy matrix increases upward.

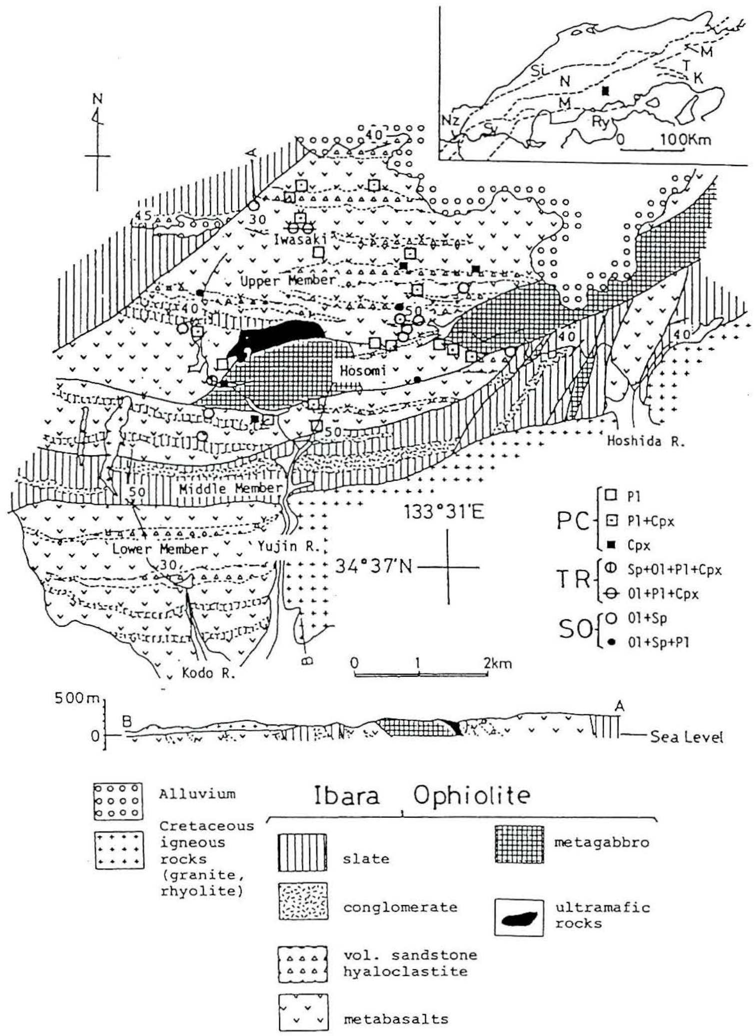

Fig. 1. Geologic map of the Ibara area and distribution of the rock types of the Upper Member porphyritic metabasalts. Abbreviations for inset. Nz: Nagato Tectonic Zone, Sy: San-yo branch of the Sangun Belt, Si: San-in branch of the Sangun Belt, Ry: Ryoke Belt, N: North Zone of the Sangun Belt, K: Kamigori Belt, T: Tamba Belt, M: Maizuru Tectonic Belt (simplified from NISHIMURA et al., 1977). The rock types of SO, TR and PC are classified by phenocryst assemblage.

Upper Member: The Upper Member, having total thickness of about 2000 m, is composed mainly of slightly vesicular metabasalts with minor amounts of hyaloclastite and black slate. Red shale and chert are rarely found. Original structures of pillow lavas, dykes and hyaloclastite are well preserved. The pillow lavas, the main constituent of the Upper Member, are commonly close-packed. Dykes are not commonly found. Black slate is less abundant in

Table 1. Mineral assemblages of the Upper Member metabasalts

rock	phenocryst	groundmass	texture	Abundance
NP type	none	pl (pseudomorph) cpx (relict) ol (pseudomorph) ore (pseudomorph) glass (altered)	glassy variolitic intergranular intersertal subophitic ophitic	61.0 %
SO type	moderately sp+ol sp+ol+pl	ol (pseudomorph) sp (relict) cpx(relict) pl (pseudomorph) ore (pseudomorph) glass (altered)	glassy variolitic	12.5 %
PC type	sparsely pl cpx pl+cpx	pl (pseudomorph) cpx (relict) ol (pseudomorph) ore (pseudomorph) glass (altered)	glassy variolitic intergranular intersertal subophitic ophitic	24.3 %
TR type	moderately sp+ol+pl+cpx	cpx (relict) pl (pseudomorph) sp (relict) ore (pseudomorph) glass (altered)	glassy intersertal variolitic	2.2 %

Abundance is obtained the numbers of specimens classified under the microscope. Abbreviations. sp: spinel, ol: olivine, pl: plagioclase, cpx: clinopyroxene, ore: oxide minerals (mainly titanomagnetite).

the lower horizon than in the upper horizon.

Metagabbro has a fine- to coarse-grained gneissose texture, and has been metamorphosed to amphibolite facies. The ultramafic rocks have wehrlitic composition but are mostly altered into serpentinite. Blocks of clinopyroxenite, ranging from one to several meters in diameter, are sometimes found in the wehrlite. No igneous layering can be observed.

III. Petrography of Metabasalts

Metabasalt from the Upper Member consists of porphyritic and non-porphyritic rocks. About 60% of the metabasalts are of the non-porphyritic one (Table 1).

The non-porphyritic (NP) metabasalt of the Upper Member has fine- to coarse-grained textures. A typical textural change can be observed within a pillow lobe as follows; glassy, variolitic, intersertal, intergranular, subophitic and ophitic from rim to core. The glassy part is commonly altered to a fine-grained aggregate of oxides and sheet silicates. The variolitic part is composed mainly of variolitic plagioclase, skeletal and dendritic clinopyroxenes, oxide minerals, and altered glass. The intersertal and intergranular parts are made up mainly of plagioclase laths, subhedral to granular clinopyroxene, oxide minerals and/or altered glass. The subophitic and ophitic parts consist of tabular plagioclase and anhedral clinopyroxene.

The porphyritic metabasalts of the Upper Member are essentially classified into the following three rock types; spinel + olivine ± plagioclase (SO), plagioclase + clinopyroxene (PC), and transitional types (TR).

Spinel + olivine ± plagioclase Type (SO type): The SO type metabasalt amounts to about 30 % of the porphyritic rocks and is moderately olivine phyric (2 ~ 10 vol.% phenocryst). This type rock contains scarcely plagioclase phenocrysts. Olivine phenocrysts include spinel. Igneous textures are preserved even though the rocks are highly altered. This type of metabasalt commonly has a glassy groundmass rich in dendritic clinopyroxene.

Plagioclase + clinopyroxene Type (PC type): The PC type metabasalt is usually sparsely phyric (<2 vol.% phenocryst) and contains phenocrysts of plagioclase and/or clinopyroxene. Plagioclase phenocrysts rarely include clinopyroxene crystals. The groundmass is similar to that of the non-porphyritic metabasalt.

Transitional Type (TR type): The TR type metabasalt comprises two phenocryst assemblages of spinel + olivine + plagioclase + clinopyroxene (TR-1) and olivine + plagioclase + clinopyroxene. The clinopyroxene phenocrysts are mostly euhedral but rarely anhedral or granular. The groundmass of this type is similar to that of both the SO and PC type metabasalts.

The major part of the metabasalt of the Lower Member has been subjected to late contact metamorphism by Cretaceous granite, and so primary igneous textures are rarely preserved.

All rock types of the porphyritic metabasalt (SO, PC and TR types) are distributed throughout the Ibara area as shown in Fig. 1. The abundance of the SO, PC and TR type metabasalts is also observed in columnar sections obtained along some routes (Fig. 2). For example, PC, NP, PC, NP, TR and PC type metabasalts occur successively from lower to upper in a continuous outcrop along the route D. Such occurrences suggest that each rock type was not derived from a tectonic slice of different magma origin, but rather the rocks were formed by a magmatism having genetic relationship.

IV. Bulk Rock Chemistry

Major element analyses were carried out using an X-ray fluorescence analyzer (JEOL Model JSX-60S7). Ni and Cr were measured by atomic absorption spectrometer (AA-475, Varian Techtron). Table 2 lists analyses of the Upper Member metabasalts of the Ibara ophiolite. New analyses of JB-1 and JG-1 are also given in Table 2, which agree fairly well with the recommended values (Ando et al., 1974).

Koide (1986; 1990) and Koide et al. (1987) have found that the Ibara metabasalts belong to the tholeiitic rock series, and are characterized by

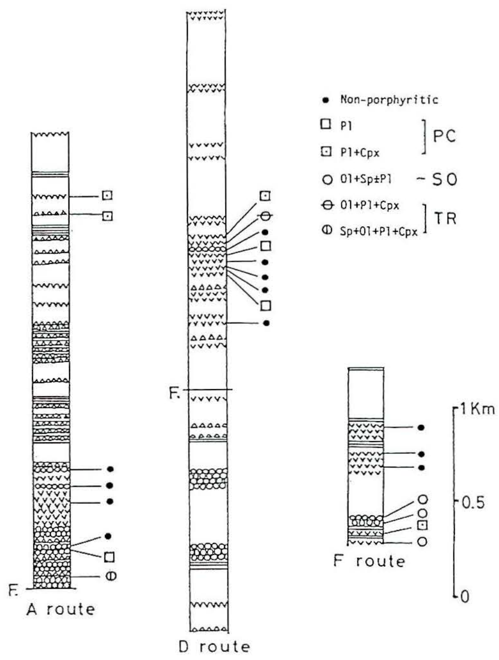

Fig. 2. Columnar sections along the A, D and F routes showing the sequence of the rock types of the Upper Member metabasalts.

1) low FeO*/MgO,
2) TiO_2 contents higher than arc tholeiites and less than ocean island tholeiites,
3) low Rb and Sr contents, and
4) high initial Nd isotope ratio.

These features correspond to chemical characteristics of MORB. However, the Ibara metabasalts have slightly higher SiO_2 contents and higher normative plagioclase contents than typical MORB. Relatively higher initial $^{87}Sr/^{86}Sr$ ratios are also characteristics of the Ibara metabasalts. These chemical characteristics suggest that the Ibara ophiolite was derived from a marginal sea mantle (KOIDE, 1990).

In MORB-like tholeiitic rocks, Ti is partitioned into clinopyroxene and Fe-Ti oxides. Since relict clinopyroxene preserves its initial chemistry, its Ti is immobile. Titanomagnetite which is another Ti-bearing mineral of the Ibara metabasalts contains exsolved magnetite and ulvospinel, the latter of which is sometimes replaced by sphene. Accordingly, Ti is fixed in sphene and ulvospinel, and was experientially not removed or leached during metamorphism and alteration.

Chromium is partitioned between clinopyroxene and spinel. Both minerals are usually preserved as relicts, so that Cr can be regarded as an immobile element.

Nickel is concentrated in olivine. In the Ibara metabasalt, however, olivine is completely altered and recrystallized to serpentine + sphene or clinozoisite + serpentine with small amounts of opaque minerals. Ni should be fixed into Ni bearing metals, sulfides, arsenides or serpentine minerals during serpentinization (KANEOKA et al., 1964, 1975; CLARK, 1969). Then

Table 2. Bulk rock compositions of the Upper Member metabasalts

No.	SO-1	SO-2	SO-3	SO-4	SO-5	TR-1	PC-1	PC-3	PC-4	PC-5	PC-6	PC-7	PC-8	PC-9	PC-10	NP-1	NP-2
SiO_2	50.79	50.89	50.35	50.70	52.86	49.64	51.20	50.98	52.19	50.99	52.09	51.77	54.25	50.42	50.22	51.04	50.78
TiO_2	0.73	0.81	0.72	0.72	0.75	1.10	1.30	1.58	2.21	1.45	1.56	1.61	2.02	1.40	2.79	1.27	1.49
Al_2O_3	14.94	14.21	14.87	15.86	15.31	15.81	14.68	14.10	14.51	14.64	13.92	14.18	12.15	15.91	14.60	14.46	13.52
FeO*	10.18	10.91	9.58	10.31	9.91	9.26	10.89	10.81	12.10	11.92	11.76	11.28	11.45	11.04	13.48	10.06	11.85
MnO	0.25	0.16	0.13	0.27	0.07	0.16	0.21	0.20	0.24	0.24	0.09	0.19	0.24	0.16	0.17	0.18	0.28
MgO	8.58	6.87	5.70	5.34	3.68	10.70	9.13	7.31	7.27	7.12	7.12	7.00	6.92	5.75	4.02	8.94	8.81
CaO	11.86	12.22	14.17	13.08	13.96	9.42	9.09	12.04	7.93	9.61	8.61	10.27	9.19	11.66	8.37	10.32	10.26
Na_2O	1.92	3.59	3.77	3.43	3.11	2.29	2.59	2.65	2.61	2.68	3.05	2.74	3.75	3.23	3.82	3.12	2.80
K_2O	0.67	0.27	0.49	0.13	0.19	1.49	0.79	0.15	0.69	1.27	1.68	0.75	0.03	0.25	1.25	0.50	0.08
P_2O_5	0.08	0.07	0.22	0.16	0.16	0.13	0.12	0.18	0.25	0.08	0.12	0.21	n.a.	0.18	0.16	0.11	0.13
Ni(ppm)	194.0	227.1	167.1	173.3	217.2	180.2	84.3	67.3	81.4	31.4	39.5	61.3	38.0	112.0	14.4	68.3	74.8
Cr(ppm)	760.1	605.8	661.2	797.7	1285.7	350.9	279.4	231.7	229.4	183.3	190.9	179.7	34.0	337.8	18.7	288.9	210.8

No.	NP-3	NP-4	NP-6	NP-7	NP-8	NP-9	NP-10	NP-11	NP-12	NP-13	NP-14	NP-16	NP-17	NP-18		JB-1#	JB-1##
SiO_2	51.38	53.59	52.15	51.52	52.58	51.55	51.94	49.69	51.36	48.45	53.24	52.08	51.53	55.55		53.47	53.39
TiO_2	1.36	1.31	1.68	1.48	1.74	1.46	1.70	2.28	2.05	2.22	2.04	1.42	1.88	1.67		1.39	1.38
Al_2O_3	13.73	13.25	13.47	14.30	11.19	14.05	13.61	15.89	14.21	14.53	12.78	15.11	14.69	14.00		14.93	14.83
FeO*	11.48	10.80	12.28	10.53	12.39	10.43	11.79	10.38	13.17	14.08	12.99	11.36	12.27	11.26		8.15	8.29
MnO	0.23	0.23	0.26	0.18	0.22	0.19	0.21	0.16	0.26	0.18	0.26	0.17	0.16	0.13		0.16	0.15
MgO	8.20	8.19	8.00	7.90	7.66	7.65	7.60	7.17	7.13	6.92	6.73	6.55	5.53	4.96		8.02	7.89
CaO	11.97	9.44	8.22	10.14	11.02	11.20	9.43	9.56	8.92	10.40	8.50	8.00	8.78	8.84		9.35	9.48
Na_2O	1.35	2.81	3.58	3.65	3.17	3.34	3.47	3.65	2.53	3.01	3.11	4.86	4.89	3.06		2.85	2.86
K_2O	0.17	0.26	0.20	0.19	0.03	n.d.	0.11	0.93	0.14	n.d.	0.15	0.30	0.27	0.37		1.43	1.46
P_2O_5	0.13	0.12	0.16	0.11	n.a.	0.13	0.14	0.29	0.23	0.21	0.20	0.15	n.a.	0.16		0.25	0.27
Ni(ppm)	58.4	56.6	41.0	65.6	31.4	54.1	48.1	96.0	29.9	32.1	30.4	56.6	32.9	28.4		198.9	135
Cr(ppm)	197.5	93.9	97.7	260.3	69.2	213.8	128.2	237.8	76.8	133.9	68.2	253.0	92.9	130.1		388.1	405

The compositions recalculated on water free basis. *: total iron as FeO, n.a.: not analysed. SO: SO type metabasalt, TR: TR type metabasalt, PC: PC type metabasalt, NP: NP type metabasalt, #: this work, ##: Ando et al. (1974).

Ni may be immobile.

In MORB-like tholeiites, TiO_2 increases, and Ni and Cr decrease with fractionation of spinel, olivine, clinopyroxene and plagioclase. Titanomagnetite occurs as a quench mineral in the groundmass of the Ibara metabasalts. Ti participated in melt as an incompatible element during fractional crystallization, whereas Cr and Ni acted as compatible elements. Accordingly, Ti, Ni and Cr are useful indicators of the extent of fractional crystallization.

The SO type metabasalt is low in TiO_2 (<1.0 wt%), and high in Cr (>600 ppm) and Ni (>160 ppm) contents (Fig. 3). On the other hand, the PC and NP type metabasalts have high TiO_2 (>1.2 wt%), and low Cr (<340 ppm, <290 ppm) and Ni contents (<120 ppm, <100 ppm, respectively). The TR type metabasalt is characterized by intermediate amounts of TiO_2 (1.1 wt%), Cr (350 ppm), and Ni (180 ppm) between the SO type, and the PC and NP types.

It is noteworthy that the PC and NP type metabasalts are similar to each other in TiO_2, Cr and Ni contents and they also have similar mineral assemblage. The PC type metabasalt contains small amounts of plagioclase and clinopyroxene phenocrysts, that is, sparsely phyric rock. The PC type metabasalt is regarded as being derived from the same magma as the NP type metabasalt. Therefore, the PC and NP type metabasalts are treated as the same rock type (PC&NP type).

V. Mineral Chemistry

Of the Ibara metabasalts, rock forming minerals are spinel, olivine, plagioclase and clinopyroxene. The chemistry of the preserved minerals provides important information on the magmatic character of the rocks. Spinel is present in the SO and TR type metabasalts, while clinopyroxene occurs in the TR and PC&NP type metabasalts.

1. Spinel

Spinel from MORB has a low Fe^{3+} content (BRYAN, 1972; RIDLEY et al., 1974; SIGURSSON and SCHILLING, 1976), and this characteristic is useful in determining magma affinity of MORB and ophiolitic basalts.

Spinel of the Ibara metabasalt occurs as microphenocryst and as minute crystal included in olivine phenocryst or in the groundmass. There is no difference in the composition among all types of spinel in the same sample (Table 3).

In the Ibara metabasalt, spinel is characterized by low $Fe^{3+}/(Cr+Al+Fe^{3+})$ (<0.1) and $Cr/(Cr+Al)$ ratios (0.4~0.5), and is similar to MORB spinel (KOIDE, 1986).

In TiO_2-$Cr/(Cr+Al)$ diagram (Fig. 4), spinel of the TR type metabasalt has a higher TiO_2 content (>0.5 wt%) than that of the SO type metabasalt (<0.5 wt%).

Fe^{3+} content of spinel in the TR type metabasalt is relatively higher than that in the SO type with the same mg value. Fe^{3+} and FeO of the SO type metabasalt (<1.2 and 7.0 wt%) are also lower than those of the TR type (>1.3 and >7.0 wt%, respectively).

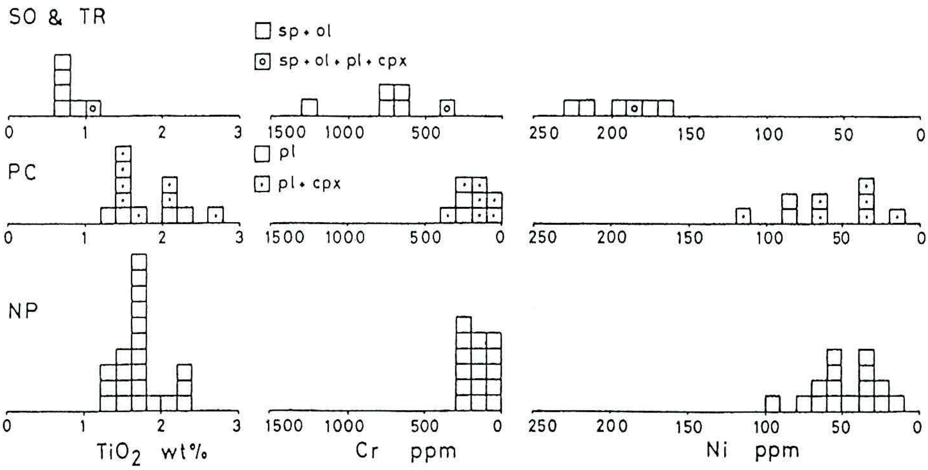

Fig. 3. TiO_2, Ni and Cr histograms of the Ibara metabasalt.

2. Clinopyroxene

Clinopyroxene Al-Si and Ti-Al diagrams (KUSHIRO, 1960) for discrimination of magmatic parentage have been widely used (e.g. LEBAS, 1962; AOKI, 1964). MARUYAMA (1976) advocated the boundaries between tholeiitic and alkaline rock series. TAKASAWA and HIRANO (1977) have also proposed the Al_2O_3-FeO diagram to discriminate rock series.

Representative clinopyroxene analyses of the Ibara metabasalt are listed in Table 4. Clinopyroxene phenocrysts from the Ibara metabasalt are characterized by high Si (1.85~1.95), low Al (0.07~0.15) and low Ti (0.01~0.03). Groundmass clinopyroxene shows

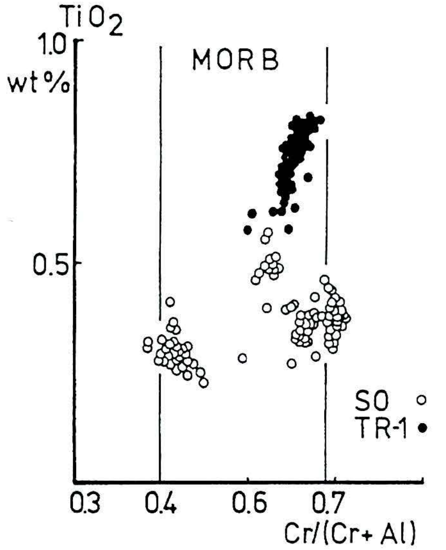

Fig. 4. TiO_2-Cr/(Cr+Al) diagram for spinels of the SO and TR type metabasalts. Compositional field of spinels from MORB are shown by two solid lines (after DICK and BULLEN, 1984).

Table 3. Representative spinel compositions

	SO-1		SO-2		SO-3		SO-4		SO-5		TR-1	
	inGM	inOL	inGM	inOL	inGM	inOL	inGM	inOL	inGM	inOL	inGM	inOL
SiO2	0.12	0.14	0.11	0.11	n.d.	n.d.	0.12	0.10	n.d.	n.d.	n.d.	n.d.
TiO2	0.37	0.39	0.48	0.50	0.39	0.34	0.31	0.28	0.38	0.45	0.77	0.75
Al2O3	22.72	22.04	24.67	24.95	23.57	22.97	31.89	30.67	20.94	20.63	21.44	21.79
Fe2O3*	4.32	4.17	4.64	4.88	6.48	6.03	3.49	5.42	5.98	5.62	7.44	7.13
FeO	12.31	17.29	14.60	15.65	12.65	12.07	12.72	12.31	14.32	12.68	15.36	15.27
MnO	0.30	0.54	0.32	0.36	0.28	0.26	0.27	0.17	0.22	0.21	0.36	0.25
MgO	14.89	12.05	13.89	13.29	14.89	15.35	15.83	16.22	13.63	14.61	13.32	13.31
CaO	0.16	0.16	0.23	0.08	0.25	0.15	0.06	0.05	0.12	0.19	0.08	0.10
Na2O	n.d.	0.01	n.d.	n.d.	n.d.	n.d.	n.d.	n.d.	n.d.	n.d.	n.d.	0.04
K2O	n.d.	0.01	n.d.	n.d.	n.d.	n.d.	n.d.	n.d.	n.d.	n.d.	n.d.	n.d.
Cr2O3	43.63	44.59	41.22	40.15	41.79	43.45	35.08	35.56	44.34	45.42	41.91	41.47
NiO	0.20	0.18	0.16	0.17	0.16	0.14	0.24	0.19	0.13	0.12	0.08	0.16
CoO	n.a.	n.a.	n.a.	n.a.	0.06	0.06	n.a.	n.a.	n.d.	0.06	n.a.	n.a.
Total	99.02	101.57	100.32	100.14	100.52	100.82	100.01	100.97	100.06	99.99	100.76	100.27
Oxygen = 32												
Si	0.028	0.033	0.026	0.026	-	-	0.028	0.023	-	-	-	-
Ti	0.067	0.072	0.088	0.092	0.070	0.062	0.054	0.049	0.070	0.082	0.142	0.139
Al	6.562	6.332	7.038	7.151	6.705	6.151	8.760	8.386	6.093	5.974	6.205	6.322
Fe^{3+}	0.795	0.765	0.845	0.893	1.177	1.093	0.612	0.946	1.111	1.038	1.376	1.322
Fe^{2+}	2.523	3.526	2.956	3.182	2.553	2.429	2.480	2.389	2.956	2.605	3.155	3.143
Mn	0.062	0.112	0.065	0.073	0.058	0.052	0.052	0.034	0.046	0.044	0.075	0.052
Mg	5.439	4.379	5.011	4.817	5.359	5.509	5.502	5.610	5.016	5.353	4.878	4.884
Ca	0.042	0.041	0.059	0.021	0.065	0.040	0.014	0.013	0.032	0.051	0.022	0.025
Na	-	0.006	-	-	-	-	-	-	-	-	-	0.018
K	-	0.002	-	-	-	-	-	-	-	-	-	-
Cr	8.453	8.595	7.889	7.719	7.977	8.269	6.465	6.524	8.656	8.823	8.136	8.073
Ni	0.029	0.026	0.024	0.025	0.023	0.020	0.034	0.026	0.020	0.017	0.012	0.023
Co	-	-	-	-	0.012	0.011	-	-	-	0.013	-	-

*: Fe2O3 is calculated by stoichiometry, inGM: spinel in groundmass, inOL: spinel in olivine, n.d.: not detected, n.a.: not analyzed.

a decreasing trend of Al_2O_3 (2 to 4 wt%) with increasing FeO (7 to 10 wt%). Therefore, the clinopyroxene chemistries of the Ibara metabasalt show a tholeiitic parentage (KOIDE, 1986).

Cores of phenocrystic clinopyroxene in the PC&NP type metabasalt are augite, while those in the TR type are endiopside (Fig. 5A). The clinopyroxene in the TR type metabasalt is richer in Mg than those of the PC&NP type.

Clinopyroxene cores in the TR type metabasalt have lower Ti contents (Fig. 5B) than 0.01 (average TiO_2 = 0.35 wt%). On the other hand, the Ti contents of the PC&NP type metabasalt exceed 0.01 ($TiO_2 > 0.4$ wt%). There is notable difference in Cr_2O_3 content between clinopyroxenes of the TR and PC&NP type metabasalts. The clinopyroxene of the TR type metabasalt is higher in Cr_2O_3 than that of the PC&NP type, which has less than 1.0 wt% (Fig. 5C).

Fig. 6 shows zoning patterns of the clinopyroxene in each rock type. The clinopyroxene of NP-3 is ophitic, and those of PC-7 and TR-1 are phenocrysts. From core to rim, the clinopyroxenes of NP-3 and PC-7 show a decrease in MgO and Cr_2O_3 with increasing FeO. These zoning is normal. The clinopyroxene of TR-1 has a complex zoning pattern for each element.

The plate shows the microprobe elemental map analyses of a clinopyroxene phenocryst from TR-1. The maps show the zone profile from rim to core of TR-1 clinopyroxene. The colors, black, blue, cyan, green, yellow, red, mazarine and white in these maps show Mg, Fe and Cr in increasing order of concentration. The complex zone of the TR type is characteristically observed in Cr map. The others show simple normal zonings. The Cr concentration from the inner to outer core changes high to low. This pattern is typical normal zoning. Whereas, the Cr concentration from the outer core to the rim becomes higher than core. Furthermore, the pattern is oscillatory. This complex zoning pattern obviously an oscillatory reverse zoning. The same patterns are observed in the Al_2O_3 and TiO_2 shown in Fig. 6.

VI. Discussion

1. Fractional crystallization

Variations of TiO_2, Cr and Ni contents suggest that the SO type metabasalt is the least fractionated, while the PC&NP type is the fairly fractionated. The TR type has intermediate degree of fractionation. The PC&NP type metabasalt shows the wide chemical variation.

The compositional variation of PC&NP type magma was controlled by fractional crystallization of olivine, plagioclase and clinopyroxene. The variation trend of PC&NP type can be interpreted by the Rayleigh fractionation model. Distribution coefficients used for calculation of the Ibara metabasalts are given in Fig. 7.

The arrows on the right sides of Cr- and Ni-TiO_2 diagrams (Fig. 7) show the fractionation trends of residual melt with proportion of crystallization of respective mineral. If the

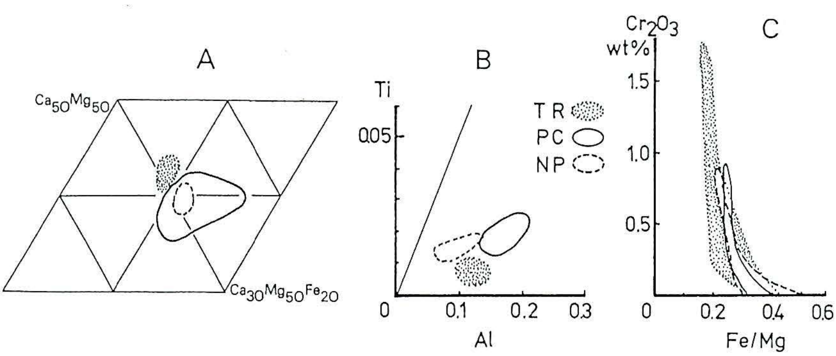

Fig. 5A, B and C. Fe-Mg-Ca, Ti-Al and Cr_2O_3-Fe/Mg diagrams for clinopyroxene of the TR, PC and NP type metabasalts. PC and NP type clinopyroxenes show core data in Fig. A and B, while that of TR type represents outer core data where the clinopyroxene equilibrates with a final liquid.

Table 4. Representative clinopyroxene compositions

	TR-1	PC-1	PC-3	PC-6		PC-7		NP-1	NP-2	NP-3	NP-4	NP-7	NP-10
	Pheno	Pheno	Pheno	inGM	Pheno	inGM	Pheno	inGM	inGM	inGM	Oph	inGM	inGM
SiO_2	52.09	50.75	49.03	49.63	50.54	52.39	48.59	51.89	52.02	50.59	48.76	51.73	50.47
TiO_2	0.35	0.75	0.52	1.34	0.64	0.58	1.69	0.42	0.42	0.54	1.07	0.45	0.68
Al_2O_3	3.07	3.55	4.78	5.49	3.48	3.20	2.60	2.11	3.53	3.24	2.29	2.11	2.90
FeO*	4.93	9.91	8.62	10.54	8.94	8.05	18.87	6.53	6.64	7.09	17.07	6.33	8.29
MnO	0.07	0.25	0.17	0.22	0.24	n.d.	0.31	0.44	0.16	0.18	0.41	0.23	0.32
MgO	16.85	17.36	15.32	14.85	17.46	19.55	8.75	17.43	16.84	17.35	12.26	18.53	16.47
CaO	21.24	17.33	19.89	16.79	17.42	16.22	18.94	20.75	19.76	20.26	18.17	20.58	19.99
Na_2O	0.19	0.18	0.26	n.d.	n.d.	0.14	0.24	n.d.	0.19	0.18	0.22	0.20	0.18
K_2O	n.d.	n.d.	n.d.	n.d.	n.d.	0.01	n.d.	n.d.	0.01	n.d.	n.d.	n.d.	n.d.
Cr_2O_3	1.22	0.08	1.06	0.02	0.10	0.32	n.d.	0.33	0.61	0.75	0.41	0.38	0.32
NiO	0.03	0.07	0.05	n.a.	n.a.	n.d.	0.02	n.a.	0.03	n.d.	n.d.	0.04	0.02
V_2O_5	n.a.	0.15	0.14	0.14	0.10	n.a.	n.a.	n.a.	0.27	n.d.	n.d.	0.06	0.09
Total	100.04	100.38	99.84	99.02	98.92	100.41	100.04	99.90	100.48	100.18	100.66	100.64	99.73
Oxygen = 6													
Si	1.905	1.873	1.829	1.857	1.886	1.903	1.891	1.915	1.898	1.866	1.870	1.893	1.879
Ti	0.010	0.021	0.015	0.038	0.018	0.016	0.050	0.012	0.012	0.015	0.031	0.013	0.019
Al	0.133	0.155	0.210	0.242	0.153	0.137	0.119	0.092	0.152	0.141	0.103	0.091	0.127
Fe	0.151	0.306	0.269	0.330	0.279	0.244	0.614	0.202	0.203	0.219	0.548	0.194	0.258
Mn	0.002	0.008	0.005	0.007	0.008	-	0.010	0.014	0.005	0.006	0.013	0.007	0.010
Mg	0.919	0.955	0.852	0.828	0.971	1.059	0.507	0.959	0.916	0.955	0.701	1.011	0.914
Ca	0.833	0.685	0.795	0.673	0.696	0.631	0.790	0.821	0.772	0.801	0.747	0.807	0.797
Na	0.014	0.013	0.018	-	-	0.010	0.018	-	0.013	0.013	0.016	0.015	0.013
K	-	-	-	-	-	0	-	-	0.001	-	-	-	-
Cr	0.035	0.003	0.031	0.001	0.003	0.009	-	0.010	0.018	0.022	0.012	0.011	0.009
Ni	0.001	0.002	0.001	-	-	-	0	-	0.001	-	-	0.001	0
V	-	0.004	0.003	0.003	0.003	-	-	-	0.006	-	-	0.001	0.002

*: total iron as FeO, Pheno: clinopyroxene as a phenocryst, inGM: clinopyroxene in groundmass, Oph: ophitic clinopyroxene, n.d.: not detected, n.a.: not analyzed.

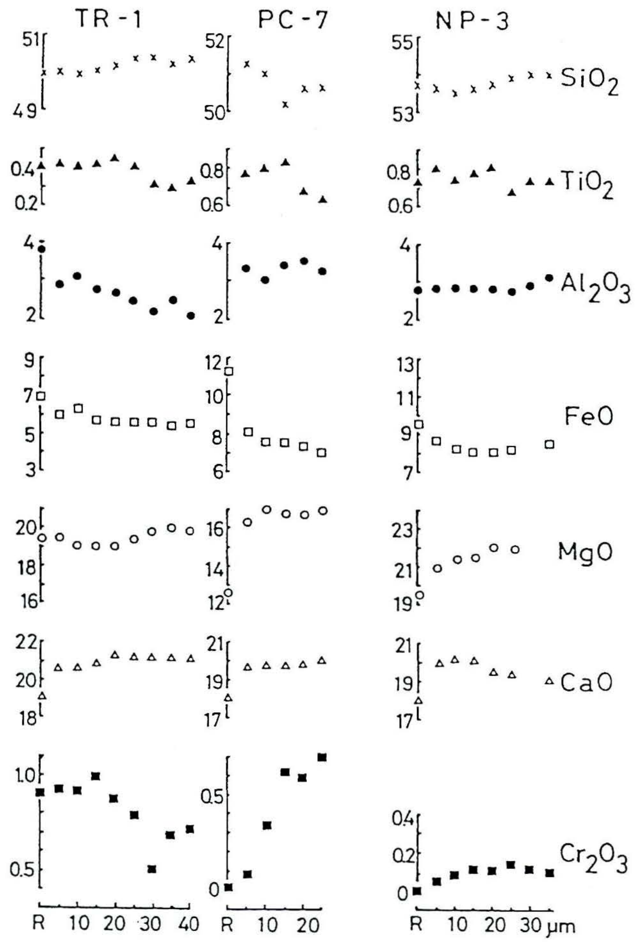

Fig. 6. Zoning patterns of clinopyroxenes of the TR, PC and NP type metabasalts. Oxide wt% versus distance (μm) from the rim (R) to core.

proportion of fractionating minerals are determined, the crystallization trend can be estimated.

The arrows in the center of Fig. 7 show the calculated trends of Rayleigh fractional crystallization. The trends are consistent with actual variation trends.

Phenocrysts of the SO type metabasalt are spinel and olivine which are sometimes accompanied by plagioclase. Fractionation of these minerals at any ratio does not follow variation trends from the SO type magma to the PC&NP type melt through the TR type. Considering fractionation of clinopyroxene, which is observed in cumulate rocks (metagabbro, wehrlite and clinopyroxenite) together with spinel, olivine and plagioclase, the variation of basaltic magma from the SO to PC&NP type metabasalt cannot be explained. For example, the calculated fractionation trends of intermediate mineral assemblage between ultramafic rocks and gabbro (olivine : spinel : clinopyroxene : plagioclase = 26 : 2 : 20 : 52 in volume percent) are shown in Fig. 7 (arrows in the left). The results are inconsistent with the actual trend. Therefore, a simple fractional crystallization model can interpret the variation trend within the PC&NP type magma, but cannot explain the trend from the SO to PC&NP type magma through the TR type magma.

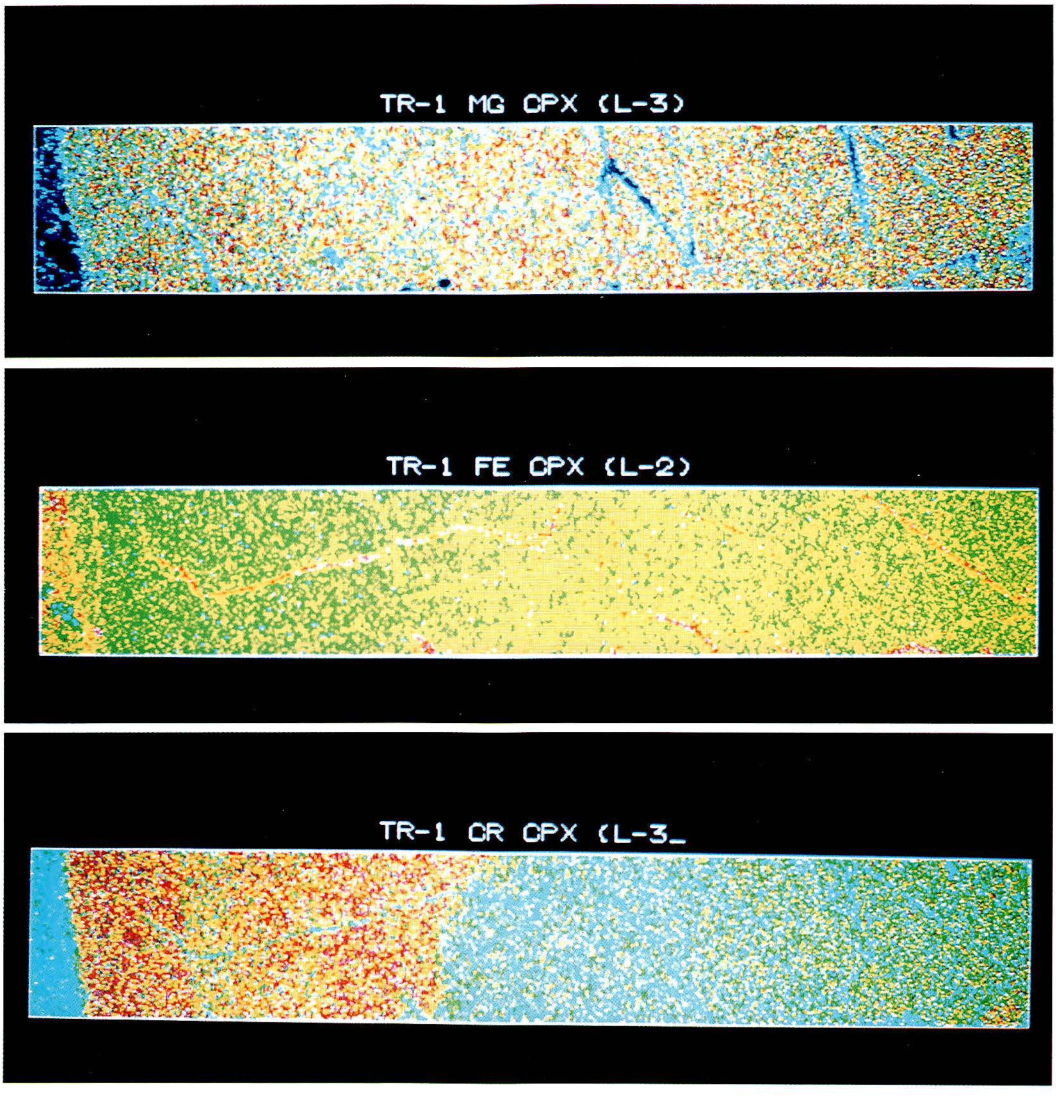

Plate. Contour maps for a clinopyroxene phenocryst of the TR type metabasalt (TR-1). These were obtained by EPMA (JXA-733). The maps are 520 μm in length and 80 μm in width. From the left to right side, the map represents the groundmass and the rim and core of a clinopyroxene phenocryst, successively. Colors show concentrations of elements; black, blue, cyan, green, yellow, red, mazarine and white, in increasing order of concentration. The upper, middle and lower of the maps are the Fe, Mg and Cr concentrations, respectively.

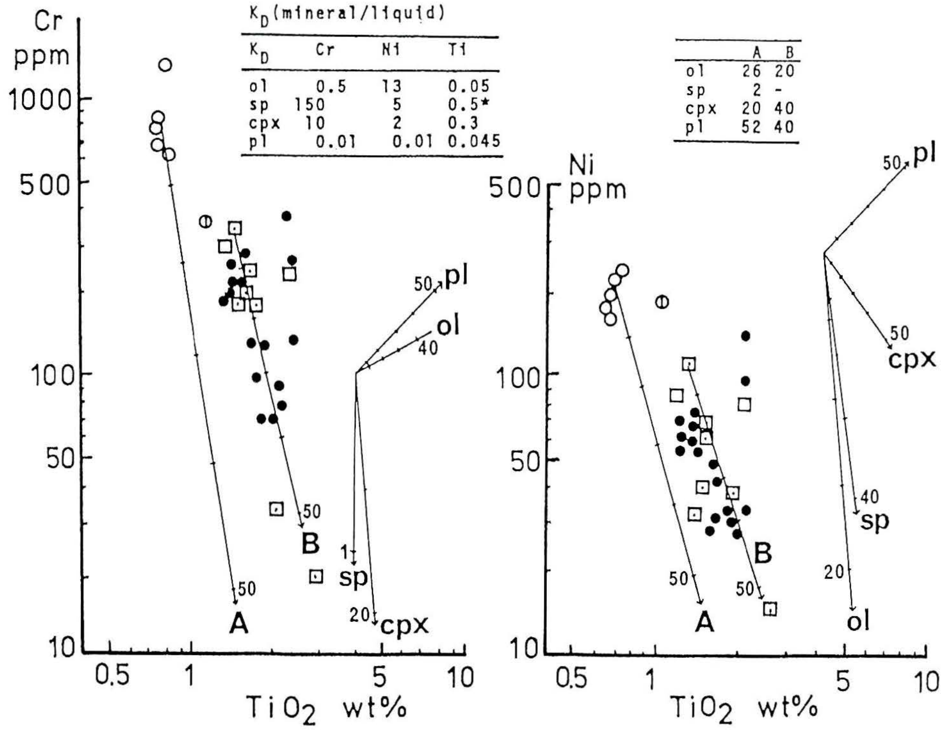

Fig. 7. Rayleigh fractionation of the Ibara metabasalt in Cr- and Ni-TiO_2 diagrams. The inset table in the Cr-TiO_2 diagram shows distribution coefficients (K_D) compiled by literature. The inset table in the Ni-TiO_2 diagram represent volume percent of fractionated minerals in two models (A and B), which show two arrows in the center of each diagram. *; data form Ibara metabasalt. Four mineral arrows in right side of each diagram show volume percent and composition trend of residual melt with fractionating each mineral. Symbols are the same as Fig. 2.

2. Magma Mixing: Evidences and Model

Evidences: The clinopyroxene phenocryst of the TR type metabasalt represents an oscillatory reverse compositional zoning from outer core to rim. Fractional crystallization model cannot account for the chemical variation among three type magmas.

Furthermore, relict mineral chemistries among three rock types show some differences. Spinel composition of the SO type metabasalt is lower TiO_2 content (<0.5 wt%) and Fe^{3+} ratio at the same mg value than those of TR type. Clinopyroxene of the TR type metabasalt is lower in Fe/Mg ratio (>0.18) and Ti content (<0.01) and higher in Cr_2O_3 content (<1.5 wt%) than those of the PC&NP type (Fe/Mg>0.20, Ti>0.01 and $Cr_2O_3<1.0$ wt%).

Factors governing spinel composition are pressure, oxygen fugacity, temperature, and magma composition (IRVINE, 1965, 1967; THOMPSON, 1973; HILL and ROEDER, 1974; SHIRAKI et al., 1979; NAGAO et al., 1980). In the Ibara metabasalts, there is no need to consider a pressure effect. Because spinel occurs as microphenocrysts in the groundmass, and crystallized at low pressure. With increasing oxygen fugacity, Fe^{3+} in spinel increases while Ti

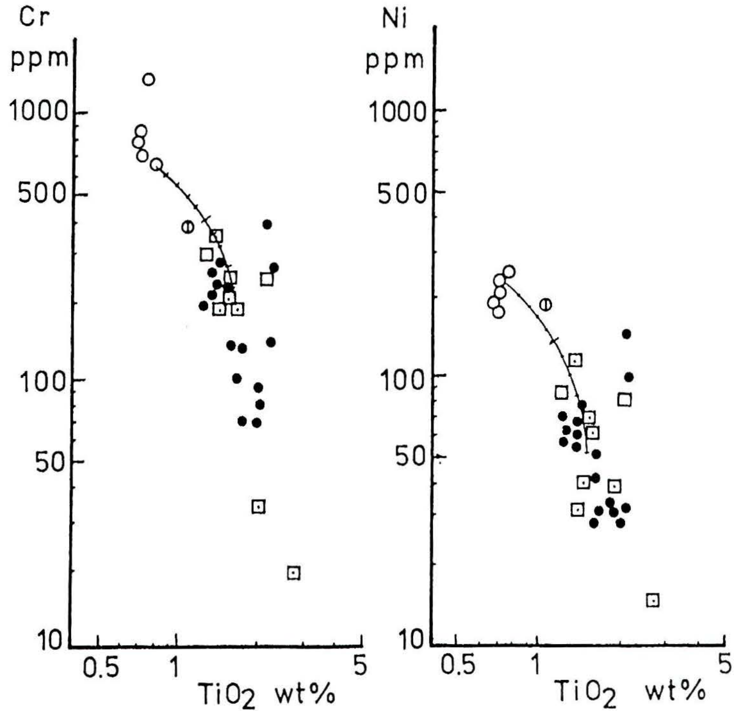

Fig. 8. Cr- and Ni-TiO_2 diagrams of mixing relations between the SO and PC&NP type magmas.

unchanged (HILL and ROEDER, 1974). This is not the case of the Ibara metabasalts. With decreasing temperature, Fe^{3+} in spinel increases and Ti increases slightly (HILL and ROEDER, 1974). This tendency is observed in the Ibara metabasalts, but the increasing degree of Ti is higher than that of Fe^{3+}. Therefore, the controlling factor of the spinel compositions in the Ibara metabasalts is neither pressure, oxygen fugacity nor temperature, but rather appears to be magma composition. TiO_2 content of the spinel of the TR type metabasalt is higher than that of the SO type. Thus the spinel of the TR type is not xenocryst derived from the SO type magma, but crystallized in equilibrium from the TR type magma.

Clinopyroxene crystallized at high pressure is characterized by high Al and low Si contents (PRESNALL et al., 1978). Clinopyroxene of the Ibara metabasalt does not have these characters, but is similar to the composition of MORB clinopyroxenes. The clinopyroxene of the Ibara metabasalt is considered to have crystallized at low pressure. The distribution coefficient of Ti between clinopyroxene and liquid generally decreases with increasing temperature (IRVING, 1978). However, both clinopyroxenes of the TR and PC&NP types have similar distribution coefficients which are nearly constant (0.30~0.45). This suggests that TiO_2 contents of clinopyroxenes of these type metabasalts are not controlled by temperature effect, but depend on magma compositions. Similarly, the Cr_2O_3 contents and mg values of the clinopyroxenes may also depend on magma composition. The clinopyroxene of the TR type metabasalt may be derived from the less fractionated magma than the PC&NP type magma.

As mentioned above, three type magmas cannot be interpreted by fractional crystallization of same magma, though the chemical variation trend within the PC&NP type metabasalt can be interpreted by fractional crystallization. Fig. 8 shows the mixing lines of the SO and PC&NP type magmas. The mixing lines connect the SO type metabasalt (SO-2) with the PC&NP type metabasalt (average values of the PC&NP type). This diagram shows that the TR type magma may have been formed by mixing between the SO and PC&NP magmas.

Model: A model of magma mixing for the Ibara metabasalts is supported by 1) oscillatory reverse zoning of clinopyroxene in the TR type metabasalt, 2) the unaccountable fractionation relationship among the SO, TR and PC&NP type magmas, 3) diversity in mineral compositions reflecting differences of their magma compositions, and 4) the TR type metabasalt having mixing composition between SO and PC&NP type magmas.

Crystallization condition can be discussed in terms of a Fo-An-Di system which is a part of the CaO-MgO-Al_2O_3-SiO_2 system. The Fo-An-Di system approximates to a basalt composition and phase relations among spinel, olivine, plagioclase and clinopyroxene can be traced in this system.

In the SO type magma, spinel, olivine and plagioclase crystallize in equilibrium. The PC&NP type magma equilibrates with plagioclase, clinopyroxene and olivine, while the TR type one is cotectic with spinel, olivine, plagioclase and clinopyroxene.

The spinel field in the Fo-An-Di diagram (Fig. 9) is narrow at 1 atm. However the addition of Cr to this system expands the spinel field (ONUMA, 1982, 1983; ONUMA and TOHARA, 1982, 1984). The Ibara metabasalt is plotted in the shaded area.

The SO and TR type metabasalts contain 0.18～0.35 and 0.10 wt% Cr_2O_3, respectively. These Cr_2O_3 contents are still effective enough to expand the spinel field, therefore spinel will crystallize from the SO and TR type magmas in equilibrium. On the other hand, the PC&NP type magma will crystallize plagioclase, clinopyroxene and olivine without spinel because of its low Cr content.

In Fig. 10, the TiO_2 content (ordinate) indicates the degree of crystallization, and Cr_2O_3 content (abscissa) controls the phase boundaries. The field enclosed by solid line shows the chemical compositional ranges of three rock types. The composition of the PC&NP type metabasalt locates in TiO_2-rich side, and that of the SO type in Cr_2O_3-rich side. The TR-1 metabasalt plots between them. The mixing process may be explained as follows: The relatively fractionated PC&NP type magma crystallizes plagioclase, clinopyroxene and olivine. On the other hand, the SO type magma, unfractionated and rich in Cr_2O_3, crystallizes spinel, olivine and plagioclase. When the SO type magma mixed with the PC&NP type magma, the mixed magma (TR-1) is enriched in Cr_2O_3 and the spinel liquidus field expands. The TR-1 magma starts crystallization of spinel and the clinopyroxene develops oscillatory reverse zoning structure.

The SO type metabasalt is observed throughout the Ibara area. This suggests that the SO type magma intermittently injected into the PC&NP type magma chamber. The TR type metabasalt alone characteristically retains clear evidence of magma mixing, and its occurrence

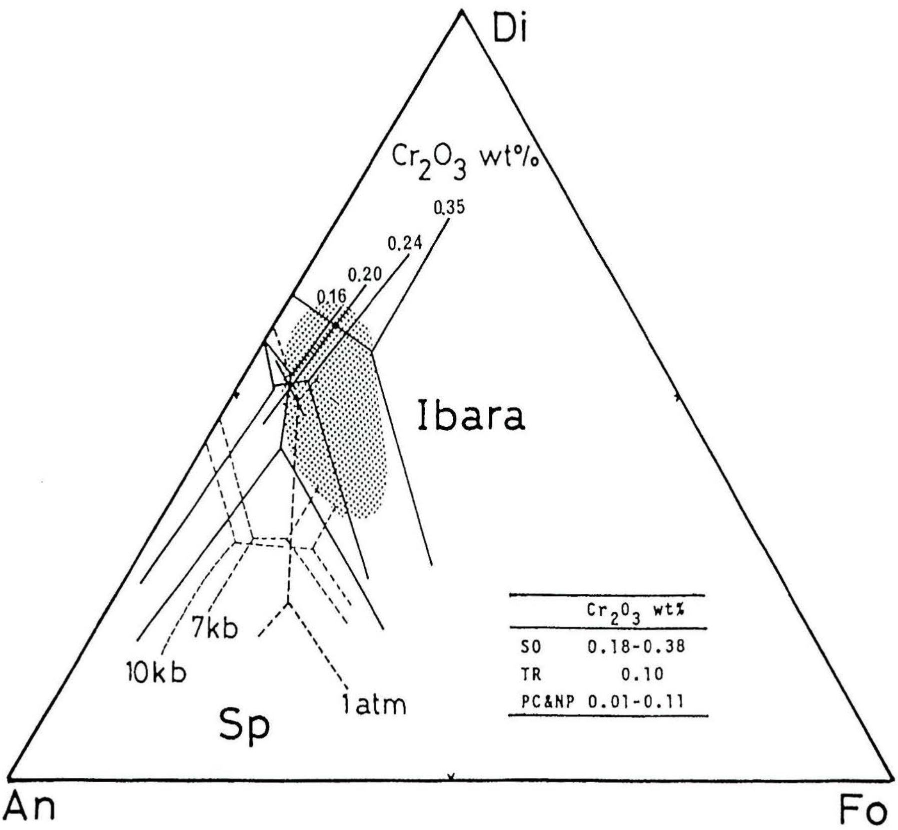

Fig. 9. Di-An-Fo diagram. The Ibara metabasalt is plotted in the shadow area. Dashed lines: phase boundaries in Cr-free system (PRESNALL et al., 1978), solid lines: Cr-bearing system (ONUMA and TOHARA, 1982; ONUMA, 1983). The inset table shows the Cr_2O_3 ranges of the Ibara metabasalt.

is rare compared with other types of metabasalts (Table 1). Therefore, it seems that the magma mixing may have been so effective that the mixing evidence has been obliterated except for the TR type metabasalt. This model is similar to open magma chamber model at modern mid-ocean ridge proposed by O'HARA (1977). The magma chamber of the Ibara ophiolite may be a "fossil" of an open magma chamber at the ridge.

VII. Conclusion

The Ibara metabasalts are MORB-like tholeiite in rock and mineral chemistries, and may have been derived from a marginal sea magmatism. Though the Ibara metabasalts have been variously metamorphosed, the crystallization process of the metabasalts has been revealed from the mineral assemblage, chemistry of relict minerals, bulk rock composition and the immobile element abundances of Ti, Cr and Ni.

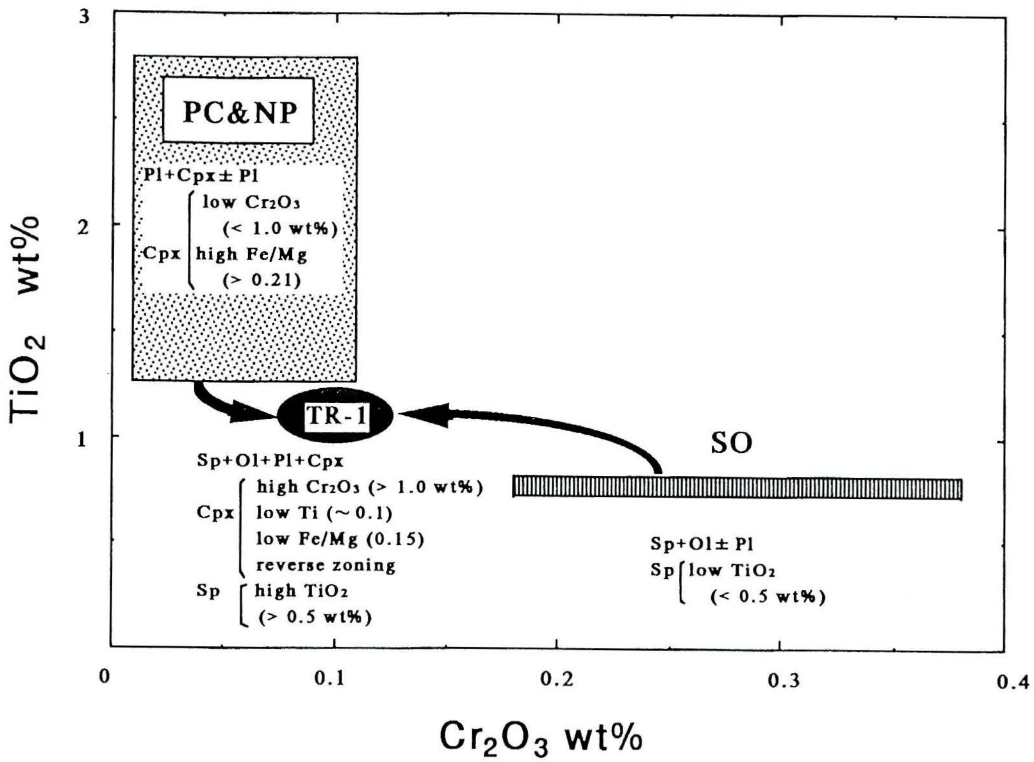

Fig. 10. TiO_2-Cr_2O_3 diagram shows genetic relation among the rock types of the Ibara metabasalt. The TR type (TR-1) represents the product of magma mixing between the SO and PC&NP type magmas.

The Ibara metabasalts are classified into three types on the basis of phenocryst assemblage; SO, TR and PC&NP. The PC&NP type magma is relatively evolved and crystallizes plagioclase, clinopyroxene and olivine. On the other hand, the SO type magma is unfractionated and rich in Cr_2O_3, and crystallizes spinel, olivine and plagioclase, while the TR type magma is intermediate between the SO and PC&NP type magmas, and crystallizes spinel, olivine, plagioclase and clinopyroxene.

Relationship among the SO, TR and PC&NP type magmas cannot be interpreted by fractional crystallization, though the variation trend in the PC&NP type metabasalt can be explained by fractionation. Differences in relict mineral chemistries of three magmas depend on their magma compositions. Clinopyroxene of the TR type metabasalt have oscillatory reverse zoning. This evidence suggests a model of magma mixing as follows; the unfractionated magma (SO type) is intermittently injected into a fractionated magma chamber (PC&NP type). The resultant mixed magma (TR type) is enriched in Cr_2O_3 and the spinel liquidus field expands. Consequently, the TR type magma begins crystallization of spinel together with plagioclase, olivine and clinopyroxene, and the clinopyroxene develops oscillatory reverse zoning structure.

Acknowledgments

The author would like to express his appreciation to Prof. K. TAZAKI of Ehime University, and Dr. K. NIIDA of Hokkaido University for many suggestions during the course of this work. He wishes to thank Prof. K. ONUMA of Tohoku University, Prof. R. GRAPES of Victoria University and Prof. S. S. SUN of research School of Earth Science, Australian National University for reading the manuscript. Thanks are also extended to people of Hokkaido University and Institute for Study of the Earth's Interior of Okayama University for valuable discussions.

References

ANDO, A., KURASAWA, H., OHMORI, T. and TAKADA, E., 1974. 1974 compilation of data on the GSJ geochemical reference samples JG-1 granodiorite and JB-1 basalt. *Geochem. Jour.*, **8**: 175–192.

AOKI, K., 1964. Clinopyroxenes from alkaline rocks of Japan. *Amer. Mineral.*, **49**: 1199–1223.

BASS, M. N., MOBERLY, R., RHODES, J. M., SHIH, C. and CHURCH, S. E., 1973. Volcanic rocks cored in the Central Pacific, Leg 17, Deep Sea Drilling Project. *Trans. Amer. Geophy. Union*, **54**: 991–995.

BRYAN, W. B., 1972. Mineralogical studies of submarine basalt. *Carnegie Inst., Washington, Year Book*, **71**: 391–403.

CARIDROIT, M., ICHIKAWA, K. and CHARVET, J., 1985. The Ultra-Tamba Zone, a new unit in the Inner Zone of Southwest Japan—its importance in the Nappe structure after the example of Maizuru Area—. *Chikyu Kagaku* (Earth Science), **39**: 210–219.

CLARK, A. H., 1969. Preliminary observations on chromian mackinawite and associated native iron, Mino do Abessedo, Vinhais, Portugal. *N. Jb. Mineral. Monatsch.*, H9: 282–288.

DICK, H. J. B., 1977. Partial melting in the Josephine Peridotite I, the effect on mineral composition and its consequence for geobarometry and geothermometry. *Amer. Jour. Sci.*, **277**: 201–230.

DICK, H. J. B. and BULLEN, T., 1984. Chromian spinel as a petrogenetic indicator in abyssal and alpine-type peridotites and spatially associated lavas. *Contrib. Miner. Petrol.*, **86**: 54–76.

DONALDSON, C. H. and BROWN, R. W., 1977. Refractory megacrysts and magnesium-rich melt inclusions within spinel in oceanic tholeiites: indicators of magma mixing and parental magma compositions. *Earth Planet. Sci. Lett.*, **37**: 81–89.

DUNGAN, M. A. and RHODES, J. M., 1978. Residual glass and melt inclusions in basalts from D.S.D.P. Legs 45 and 46: evidence for magma mixing. *Contrib. Mineral. Petrol.*, **67**: 417–431.

HASE, A., 1964. Paleozoic. *In*: Explanatory of the geological map, "Hiroshima Ken": 31–59 (in Japanese with English).

HASHIMOTO, M., 1972. Relic clinopyroxenes of Paleozoic greenstones of the Tamba and Mikabu Terrains, Southwest Japan. *Jour. Japan. Assoc. Mineral. Petrol. Econ. Geol*, **67**: 323–331 (in Japanese with English abstract).

HASHIMOTO, M. and SAITO, Y., 1970. Metamorphism of Paleozoic greenstones of the Tamba plateau, Kyoto Prefecture. *Jour. Geol. Soc. Japan*, **76**: 1–6 (in Japanese with English abstract).

HILL, R. and ROEDER, P., 1974. The crystallization of spinel from basaltic liquid as a function of oxygen fugacity. *Jour. Geol.*, **82**: 709–729.

IRVINE, T. N., 1965. Chromian spinel as a petrogenetic indicator, Part 1. Theory. *Can. Jour. Earth Sci.*, **2**: 648–672.

IRVINE, T. N., 1967. Chromian spinel as a petrogenetic indicator, Part 2. Petrologic applications. *Can. Jour. Earth Sci.*, **4**: 71–103.

IRVING, A. J., 1978. A review of experimental studies of crystal/liquid trace element partitioning. *Geochim. Cosmochim. Acta*, **42**: 743–770.

ISHIGA, H., 1983. Two suites of stratigraphic succession within the Tamba Group in the western part of the Tamba Belt, southwest Japan. *Jour. Geol. Soc. Japan*, **89**: 443–454 (in Japanese with English).

ISHIGA, H., 1985a. Age and geologic structure of Paleozoic—Mesozoic Formations in Tamba Belt, Southwest Japan. *Chikyu Kagaku* (Earth Science), **30**: 31–43 (in Japanese with English abstract).

ISHIGA, H., 1985b. Discovery of Permian radiolarians from Katsumi and Oi Formations along south of Maizuru Belt, Southwest Japan and its significance. *Chikyu Kagaku* (Earth Science), **39**: 175–185.

ISHIGA, H., 1986a. Ultra-Tamba Zone of Southwest Japan. *Jour. Geosci. Osaka City Univ.*, **29**: 45–88.

ISHIGA, H., 1986b. Late Carboniferous and Permian radiolarian Biostratigraphy of Southwest Japan. *Jour. Geosci. Osaka City Univ.*, **29**: 89–100.

KANEHIRA, K., BANNO, S. and HASHIMOTO, M., 1964. Notes on rock-forming minerals (28). Finding of awaruite (native nickel-iron) from serpentinized peridotite from the Mineoka district, south Boso Peninsula. *Jour. Japan. Assoc. Mineral. Petrol. Econ. Geol.*, **70**: 388–394.

KANEHIRA, K., BANNO, S. and YUI, S., 1975. Awaruite, heazlewoodite, and native copper in serpentinized peridotite from the Mineoka district, southern Boso Peninsula. *Jour. Japan. Assoc. Mineral. Petrol. Econ. Geol.*, **70**: 388–394.

KOIDE, Y., 1986. Origin of the Ibara metabasalts from the Maizuru Tectonic Belt, Southwest Japan. *Jour. Geol. Soc. Japan*, **92**: 329–348.

KOIDE, Y., 1990. Marginal sea ophiolite (Ibara Ophiolite) in the Southwest Japan. *In*: Proceedings of Ophiolite and Oceanic Lithosphere, Cyprus Geological Survey Department, 477–484.

KOIDE, Y., TAZAKI, K. and KAGAMI, H., 1987. Sr isotopic study of Ibara dismembered ophiolite from the Maizuru Tectonic Belt, Southwest Japan. *Jour. Japan. Assoc. Mineral. Petrol. Econ. Geol.*, **82**: 1–15.

KUSHIRO, I., 1960. Si-Al relation in clinopyroxenes from igneous rock. *Amer. Jour. Sci.*, **258**: 548–554.

LEBAS, M. J., 1962. The role of aluminum in igneous clinopyroxenes with relation to their parentage. *Amer. Jour. Sci.*, **260**: 267–288.

MACDONALD, G. and KATSURA, T., 1964. Chemical composition of Hawaiian lavas. *Jour. Petrol.*, **5**: 82–133.

MARUYAMA, S., 1976. Chemical natures of the Sawadani greenstone complex in Chichibu Belt, Eastern Shikoku. *Jour. Geol. Soc. Japan*, **82**: 183–197 (in Japanese with English).

MIYASHIRO, A., 1975. Classification, characteristic, and origin of ophiolites. *Jour. Geol.*, **83**: 249–281.

NAGAO, T., YAMAMOTO, M. and ONUMA, K., 1980. Crystallization trend of chromian spinel in some alkali basalts and calc-alkali andesites from Japanese Islands. *Jour. Japan. Assoc. Miner. Petrol. Econ. Geol.,* **75**: 44–54.

NISHIMURA, Y., INOUE, T. and YAMAMOTO, H., 1977. Sangun Belt, with special reference to the stratigraphy and metamorphism. *In*: K. HIDE (*editor*), The Sanbagawa Belt. 257–282, Hiroshima Univ. Press, Hiroshima (in Japanese with English).

O'HARA, M. J., 1977. Geochemical evolution during fractional crystallization of a periodically refilled magma chamber. *Nature,* **366**: 503–507.

ONUMA, K., 1982a. Phase relations in the $CaMgSi_2O_6$-rich part of the join $CaMgSi_2O_6$-$MgCr_2O_4$ in air at 1 atm. *Jour. Japan. Assoc. Mineral. Petrol. Econ. Geol.,* **77**: 356–361.

ONUMA, K., 1982b. The Join forsterite-anorthite-diopside with 0.3 wt% $MgCr_2O_4$ at 1 atm and its petrologic significance: a preliminary report. *Jour. Japan. Assoc. Mineral. Petrol. Econ. Geol.,* **77**: 403–409.

ONUMA, K., 1983. Phase relations in the chromium-poor part of the system diopside-anorthite-forsterite-$MgCr_2O_4$ in air 1 atm. *Jour. Fac. Sci., Hokkaido Univ.,* **20**: 171–183.

ONUMA, K. and TOHARA. T., 1981. Clinopyroxenes and spinels in the system $CaMgSi_2O_6$-$CaAl_2SiO_6$-$CaCrAlSiO_6$: a preliminary report. *Jour. Fac. Sci., Hokkaido Univ.,* **19**: 495–503.

ONUMA, K. and TOHARA, T., 1982. Effect of chromium on the phase relation in the system CaO-MgO-Al_2O_3-SiO_2. *Jour. Japan. Assoc. Mineral. Petrol. Econ. Geol.,* special issue, **3**: 195–202. (in Japanese with English abstract)

PEARCE, T. H., GORMAN, B. E. and BIRKETT, T. C., 1975. The TiO_2-K_2O-P_2O_5 diagram; a method of discriminating between oceanic and non-oceanic basalt. *Earth Planet. Sci. Lett.,* **24**: 419–426.

PEARCE, T. H., GORMAN, B. E. and BIRKETT, T. C., 1977. The relationship between major element chemistry and tectonic environment of basic and intermediate volcanic rocks. *Earth Planet. Sci. Lett.,* **36**: 121–132.

PRESNALL, D. C., DIXON, S. A., DIXON, JR., O'DONNELL, T. H., BRENNER, N. L., SCHROCK, R. L. and DYCUS, D. W., 1978. Liquidus phase relations on the join diopside-forsterite-anorthite from 1 atm to 20 kbar: their bearing on the generation and crystallization of basaltic magma. *Contrib. Mineral. Petrol.,* **66**: 203–220.

RHODES, J. M., DUNGAN, M. A., BLANCHARD, D. P. and LONG, P. E., 1979. Magma mixing at mid-ocean ridges: evidence from basalts drilled near 22° N on the Mid-Atlantic Ridge. *Tectonophy.,* **55**: 35–62.

RIDLEY, W. I., RHODES, J. M., JAKES, P., SHIH, C. and BASS, M. N., 1974. Basalt from Leg 6 of the Deep Sea Drilling Project. *Jour. Petrol.,* **15**: 140–159.

RIDLEY, W. I. and AJDUKIEWICZ, J., 1976. Preliminary petrology of Leg 34 basalts from the Nazca plate. *Initial Reports DSDP.,* **34**: 277–282.

SHIRAKI, K., OHASHI, F. and KURODA, U., 1979. Chrome-spinels in a basanitic lava from Nanzaki volcano, Izu Peninsula. *Jour. Japan. Assoc. Mineral. Petrol. Econ. Geol.,* **74**: 114–121 (in Japanese with English abstract).

SIGURSSON, H. and SCHILLING, J. G., 1976. Spinels in Mid-Atlantic Ridge basalts: chemistry and occurrence. *Earth Planet. Sci. Lett.,* **29**: 7–20.

TAKASAWA, K. and HIRANO, H., 1977. Some considerations on the relations between magma series and Al_2O_3 variation of Ca-pyroxene. *Jour. Geol. Soc. Japan,* **83**: 583–591 (in Japanese with English).

THOMPSON, R. N., 1973. Titanian chromite and chromian titano magnetite from a Snake River plain basalt, a terrestrial analogue to lunar spinels. *Amer. Mineral.,* **58**: 826–830.

WALKER, D., SHIBATA, T. and DELONG, S. E., 1979. Abyssal tholeiites from the Oceanographer Fracture Zone. II. Phase equilibria and mixing. *Contrib. Mineral. Petrol.,* **70**: 111–125.

YODER, H. S. and TILLEY, C. E., 1962. Origin of basalt magma: an experimental study of natural and synthetic rock systems. *Jour. Petrol.,* **3**: 342–532.